Iranian Journal of Astronomy and Astrophysics

Online ISSN: 2383–403X

Research Paper

Thermodynamics and Multi-Horizon Solutions in Quartic Quasitopological Gravity: A Power-Maxwell Approach

Afsaneh Bazrafshan 1 · Mohammad Ghanaatian *2 · Parviz Mirsalari 3 · Ghasem Forozani 4

- Department of Physics, Jahrom University, Jahrom, P.O. Box 74137–66171, Iran; E-mail: abazrafshan@jahromu.ac.ir
- Department of Physics, Jahrom University, Jahrom, P.O. Box 74137–66171, Iran;
 *E-mail: mghanaatian@jahromu.ac.ir; m.ghanaatian@gmail.com
- Department of Physics, Payame Noor University (PNU), P.O. Box 19395–3697, Tehran, Iran; E-mail: parvizmirsalari@student.pnu.ac.ir
- Department of Physics, Payame Noor University (PNU), P.O. Box 19395–3697, Tehran, Iran; E-mail: forozani@pnu.ac.ir

Received: 5 August 2025; Accepted: 22 October 2025; Published: 12 November 2025

Abstract. We derive exact black hole solutions in (n+1)-dimensional fourth-order quasitopological gravity (4QTG) coupled to power-Maxwell electrodynamics. Thermodynamic properties (entropy, temperature, electric potential) are analyzed, verifying the first law. Crucially, thermal stability is exclusively achievable in asymptotically AdS spacetimes, while dS and flat solutions exhibit universal instability. The study reveals that 4QTG supports multi-horizon black holes even without charge—a feature absent in Einstein gravity—due to repulsive effects of quartic curvature terms. These results highlight the role of higher-curvature corrections in resolving classical limitations of general relativity and provide new insights for AdS/CFT correspondence.

Keywords: Black Hole, Quasitopological Gravity, Power-Maxwell Field.

1 Introduction

The pursuit of a consistent quantum theory of gravity has motivated extensive research into higher-curvature extensions of Einstein's general relativity [1,2]. These theories, which emerge naturally from string theory compactifications [3] and quantum gravity considerations, introduce curvature corrections that can resolve classical singularities and significantly modify black hole thermodynamics [4–6]. Among these extensions, quasitopological gravity is particularly notable. It generates non-trivial, ghost-free dynamics in four dimensions while maintaining second-order field equations for spherically symmetric configurations [5], thus avoiding the Boulware-Deser instability common in generic higher-derivative theories [7].

Fourth-order quasitopological gravity (4QTG) represents a significant extension beyond the well-studied Einstein-Gauss-Bonnet and cubic quasitopological models by incorporating quartic curvature invariants [6]. These terms fundamentally alter the spacetime geometry, enabling several intriguing features: (1) the resolution or softening of central singularities [8],

This is an open access article under the CC BY license.





 $^{^*} Corresponding \ author$

(2) the existence of multi-horizon black hole solutions even in the absence of electric charge [9], and (3) modified conformal anomalies in the holographic dual field theory [10]. Unlike Lovelock gravity, which requires higher dimensions for its dynamics to become non-trivial [1], 4QTG operates effectively in 4D, making it a valuable framework for exploring quantum gravity phenomenology in a more realistic setting [11].

Further developments in this area include the construction of various black hole solutions within quasitopological gravity. Charged black holes were studied in [12–14], with their thermodynamic analysis revealing novel phase structures and critical behavior. Specifically, [12] derived the necessary surface terms and conserved quantities for rotating branes. Lifshitz black holes within this framework were investigated in [15], and extensions incorporating Born-Infeld nonlinear electrodynamics were explored in [13,14]. Furthermore, the physical and thermodynamic properties of quartic quasitopological black holes coupled to nonlinear sources have been extensively analyzed in [6,16,17].

A crucial advancement presented in this work is the coupling of 4QTG with power-Maxwell electrodynamics, governed by the Lagrangian density $\mathcal{L}(F) = (-F)^s$ [18,19]. This nonlinear generalization introduces a scale-dependent behavior that preserves conformal invariance in d = 2s + 1 dimensions [20], modifies black hole phase transitions [21], and can enable singularity resolution in ways distinct from Born-Infeld models [22]. The synergy between the geometric complexities of 4QTG and the scale-invariant properties of power-Maxwell electrodynamics creates a rich framework for exploring advanced gravitational thermodynamics via the AdS/CFT correspondence [23].

While multi-horizon solutions have previously been obtained in theories coupling non-linear electrodynamics (NED) to Einstein gravity [9], our analysis demonstrates that 4QTG alone, even without additional nonlinear sources, is sufficient to generate such geometries. We systematically explore the conditions under which multiple horizons emerge by analyzing the roots of the metric function, providing both analytic and numerical evidence.

This study advances previous works in five significant directions:

- 1. We derive exact (n + 1)-dimensional black hole solutions, extending previous results for cubic quasitopological gravity [17].
- 2. We demonstrate the existence of charge-independent multi-horizon solutions, generalizing observations made in NED couplings [9].
- 3. We establish comprehensive thermal stability criteria through a detailed analysis of the parameter space.
- 4. We quantify the effects of quartic curvature terms on holographic entanglement entropy and conformal anomalies [26].
- 5. We identify new phase transitions within the extended thermodynamic phase space [27].

This paper is organized as follows. In Section 2, we present the action and derive the field equations, subsequently obtaining exact black hole solutions and discussing their horizon structure. Thermodynamic properties and the first law are discussed in Section 3, where we also analyze thermal stability via the Hessian matrix formalism. Section 4 summarizes our results and outlines future research directions.

2 Field Equations and Exact Solutions

2.1 Action and Lagrangian

We begin by considering a static, (n+1)-dimensional spacetime. The action for fourth-order quasitopological gravity (4QTG) coupled to a power-Maxwell field is given by:

$$\mathcal{I} = \frac{1}{16\pi} \int d^{n+1}x \sqrt{-g} \left[-2\Lambda + \mathcal{L}_1 + \mu_2 \mathcal{L}_2 + \mu_3 \mathcal{X}_3 + \mu_4 \mathcal{X}_4 + (-F)^s \right], \tag{1}$$

where $\Lambda = -n(n-1)/(2l^2)$ is the cosmological constant, $\mathcal{L}_1 = R$ is the Ricci scalar, \mathcal{L}_2 is the Gauss-Bonnet Lagrangian, \mathcal{X}_3 and \mathcal{X}_4 are the cubic and quartic quasitopological Lagrangians, respectively, and $F = F_{\mu\nu}F^{\mu\nu}$ is the Maxwell invariant. The explicit forms of the quasitopological terms are:

$$\mathcal{X}_{3} = R_{ab}^{cd} R_{cd}^{e f} R_{e f}^{a b} + \frac{1}{(2n-1)(n-3)} \left(\frac{3(3n-5)}{8} R_{abcd} R^{abcd} R -3(n-1) R_{abcd} R^{abc}{}_{e} R^{de} + 3(n+1) R_{abcd} R^{ac} R^{bd} +6(n-1) R_{a}{}^{b} R_{b}{}^{c} R_{c}{}^{a} - \frac{3(3n-1)}{2} R_{a}{}^{b} R_{b}{}^{a} R + \frac{3(n+1)}{8} R^{3} \right), \tag{2}$$

$$\mathcal{X}_{4} = c_{1}R_{abcd}R^{cdef}R^{hg}{}_{ef}R_{hg}{}^{ab} + c_{2}R_{abcd}R^{abcd}R_{ef}R^{ef} + c_{3}RR_{ab}R^{ac}R_{c}{}^{b} + c_{4}(R_{abcd}R^{abcd})^{2}
+ c_{5}R_{ab}R^{ac}R_{cd}R^{db} + c_{6}RR_{abcd}R^{ac}R^{db} + c_{7}R_{abcd}R^{ac}R^{be}R^{d}{}_{e} + c_{8}R_{abcd}R^{acef}R^{b}{}_{e}R^{d}{}_{f}
+ c_{9}R_{abcd}R^{ac}R_{ef}R^{bedf} + c_{10}R^{4} + c_{11}R^{2}R_{abcd}R^{abcd} + c_{12}R^{2}R_{ab}R^{ab}
+ c_{13}R_{abcd}R^{abef}R_{ef}{}_{a}^{c}R^{dg} + c_{14}R_{abcd}R^{aecf}R_{gehf}R^{gbhd},$$
(3)

where the coefficients c_1 to c_{14} are dimension-dependent constants [4,6,12,13]. The electromagnetic tensor is defined as $F_{\mu\nu} = \partial_{\mu}A_{\nu} - \partial_{\nu}A_{\mu}$, with A_{μ} being the vector potential. For the purpose of finding static solutions, we choose the ansatz $A_{\mu} = h(\rho)\delta_{\mu}^{0}$.

2.2 Metric Ansatz and Equations of Motion

We assume a static metric ansatz in terms of the radial coordinate ρ :

$$ds^{2} = -\frac{\rho^{2}}{l^{2}}f(\rho)dt^{2} + \frac{l^{2}}{\rho^{2}g(\rho)}d\rho^{2} + \frac{\rho^{2}}{l^{2}}\sum_{i=1}^{n-1}d\phi_{i}^{2}.$$
 (4)

Varying the action with respect to the metric $g_{\mu\nu}$ and the vector potential A_{μ} yields the field equations. After substantial algebra, these equations simplify to:

$$(-\hat{\mu}_0 + 2\hat{\mu}_2 g + 3\hat{\mu}_3 g^2 + 4\hat{\mu}_4 g^3)N' = 0, (5)$$

$$\left\{ (n-1)\rho^{n} \left(\hat{\mu}_{0} - g + \hat{\mu}_{2}g^{2} + \hat{\mu}_{3}g^{3} + \hat{\mu}_{4}g^{4} \right) \right\}' = 2^{s}(2s-1)\rho^{n-1}l^{2} \left(\frac{h'}{N} \right)^{2s}, \tag{6}$$

$$\left(\rho^{n-1} \left(\frac{h'}{N}\right)^{2s-1}\right)' = 0,\tag{7}$$

where the dimensionless parameters $\hat{\mu}_2$, $\hat{\mu}_3$, and $\hat{\mu}_4$ are related to the original couplings μ_i and the cosmological length scale l [4]. From Eq. (5), we find that $N(\rho)$ must be a constant,

which we set to $N(\rho) = 1$ without loss of generality. Solving Eq. (7) for the electric potential $h(\rho)$ then yields:

$$h(\rho) = \begin{cases} q \ln(\rho), & s = n/2 \\ -q \rho^{-(n-2s)/(2s-1)}, & 1/2 < s < n/2 \end{cases}$$
 (8)

Here, q is an integration constant related to the electric charge. The interval 1/2 < s < n/2 is chosen to ensure the potential remains finite at spatial infinity.

Substituting $h(\rho)$ into Eq. (6) leads to a key algebraic equation for the metric function $g(\rho)$:

$$\hat{\mu}_4 g^4 + \hat{\mu}_3 g^3 + \hat{\mu}_2 g^2 - g + \kappa = 0, \tag{9}$$

where the function $\kappa(\rho)$ encapsulates the mass and charge contributions:

$$\kappa(\rho) = \hat{\mu}_0 - \frac{m}{\rho^n} + \frac{2^s l^2 q^{2s} (n-2s)^{2s-1}}{(n-1)(2s-1)^{(2s-2)} \rho^{2s(n-1)/(2s-1)}}.$$
(10)

The integration constant m represents the geometrical mass of the black hole, expressible in terms of the horizon radius ρ_+ :

$$m = \left(1 + \frac{2^{s} l^{2} q^{2s} (n - 2s)^{2s - 1} (\rho_{+})^{2s(1 - n)/(2s - 1)}}{(n - 1)(2s - 1)^{(2s - 2)}}\right) \rho_{+}^{n}.$$
 (11)

2.3 Exact Solutions for the Metric Function

The metric function $f(\rho) = g(\rho)$ is determined by solving the quartic algebraic equation (9). The four roots of this equation can be found exactly. We focus on the two physically relevant real branches, denoted $f_1(\rho)$ and $f_2(\rho)$, which correspond to different branches of the solution. They are given by:

$$f_1(\rho) = \left(-\frac{\hat{\mu}_3}{4\hat{\mu}_4} + \frac{1}{2}R - \frac{1}{2}E\right),\tag{12}$$

$$f_2(\rho) = \left(-\frac{\hat{\mu}_3}{4\hat{\mu}_4} - \frac{1}{2}R + \frac{1}{2}K\right),\tag{13}$$

where the auxiliary functions R, E, and K are defined as:

$$R = \left(\frac{\hat{\mu}_3^2}{4\hat{\mu}_4^2} - \frac{\hat{\mu}_2}{\hat{\mu}_4} + y_1\right)^{1/2},\tag{14}$$

$$E = \left(\frac{3\hat{\mu}_3^2}{4\hat{\mu}_4^2} - \frac{2\hat{\mu}_2}{\hat{\mu}_4} - R^2 - \frac{1}{4R} \left[\frac{4\hat{\mu}_2\hat{\mu}_3}{\hat{\mu}_4^2} - \frac{8\kappa}{\hat{\mu}_4} - \frac{\hat{\mu}_3^3}{\hat{\mu}_4^3} \right] \right)^{1/2}, \tag{15}$$

$$K = \left(\frac{3\hat{\mu}_3^2}{4\hat{\mu}_4^2} - \frac{2\hat{\mu}_2}{\hat{\mu}_4} - R^2 + \frac{1}{4R} \left[\frac{4\hat{\mu}_2\hat{\mu}_3}{\hat{\mu}_4^2} - \frac{8\kappa}{\hat{\mu}_4} - \frac{\hat{\mu}_3^3}{\hat{\mu}_4^3} \right] \right)^{1/2}.$$
 (16)

The term y_1 is the real root of the following cubic equation:

$$y^{3} - \frac{\mu_{2}y^{2}}{\mu_{4}} + \left(\frac{\mu_{3}}{\mu_{4}^{2}} - 4\frac{\kappa}{\mu_{4}}\right)y - \frac{\mu_{3}^{2}\kappa}{\mu_{4}^{3}} + \frac{4\mu_{2}\kappa}{\mu_{4}^{2}} - \frac{1}{\mu_{4}^{2}} = 0.$$
 (17)

These solutions, while algebraically complex, are the exact analogs of the well-known Ferrari solution for quartic equations. They are necessary to capture the full dynamics introduced by the quartic quasitopological term. For the uncharged case (q = 0), κ is a simple function

of ρ , and $f(\rho)$ is real for all $\rho \geq 0$. However, for $q \neq 0$, the function $\kappa(\rho)$ and consequently $f(\rho)$ may become complex for small ρ ($\rho < r_0$), indicating a breakdown of the ρ coordinate. To obtain a real metric for all $r \geq 0$, we perform a coordinate transformation, introducing a new radial coordinate r defined by:

$$r = \sqrt{\rho^2 - r_0^2}$$
, which implies $d\rho^2 = \frac{r^2}{r^2 + r_0^2} dr^2$. (18)

Here, r_0 is chosen as the largest real root of the equation $f(\rho) = 0$ (i.e., the innermost horizon) or where the metric becomes complex, ensuring the new coordinate r covers the entire spacetime exterior to r = 0. In this new coordinate system, the metric becomes:

$$ds^{2} = -\frac{(r^{2} + r_{0}^{2})g(r)dt^{2}}{l^{2}} + \frac{r^{2}l^{2}dr^{2}}{g(r)(r^{2} + r_{0}^{2})} + \frac{(r^{2} + r_{0}^{2})}{l^{2}} \sum_{i=1}^{n-1} d\phi_{i}^{2},$$
(19)

and the functions h(r) and $\kappa(r)$ transform accordingly:

$$h(r) = -q(r^2 + r_0^2)^{(2s-n)/(4s-2)}, (20)$$

$$\kappa(r) = \hat{\mu}_0 - \frac{m}{(r^2 + r_0^2)^{n/2}} + \frac{2^s l^2 q^{2s} (n - 2s)^{2s - 1}}{(n - 1)(2s - 1)^{(2s - 2)} (r^2 + r_0^2)^{s(n - 1)/(2s - 1)}}.$$
 (21)

The metric function g(r) (replacing $g(\rho)$) is still determined by solving Eq. (9) with κ now given by Eq. (26). This formulation ensures the metric is real and well-defined for all $r \geq 0$.

2.4 Asymptotically dS and AdS Spacetimes

The asymptotic behavior $(r \to \infty)$ of the metric function f(r) = g(r) determines the global structure of the spacetime. For asymptotically de Sitter (dS) spacetimes, we require:

$$\lim_{r \to \infty} f(r) = -1. \tag{22}$$

This condition leads to an expression for the cosmological constant:

$$\Lambda = \frac{n(n-1)}{2l^2}(\hat{\mu}_4 - \hat{\mu}_3 + \hat{\mu}_2 + 1), \tag{23}$$

where $\Lambda > 0$ requires $\hat{\mu}_4 - \hat{\mu}_3 + \hat{\mu}_2 > -1$. For asymptotically Anti-de Sitter (AdS) spacetimes, we require:

$$\lim_{r \to \infty} f(r) = 1,\tag{24}$$

which yields:

$$\Lambda = \frac{n(n-1)}{2l^2}(\hat{\mu}_4 + \hat{\mu}_3 + \hat{\mu}_2 - 1), \tag{25}$$

with $\Lambda < 0$ requiring $\hat{\mu}_4 + \hat{\mu}_3 + \hat{\mu}_2 < 1$. These conditions ensure the solutions possess the correct asymptotic behavior consistent with observational constraints on Λ [2].

The horizon structure for these asymptotic cases is illustrated in Figures 1 and 2. For dS spacetime (Figures 1), the solution exhibits a single cosmological horizon for all values of the mass parameter m. The horizon radius increases with mass, approximately following $r_+ \propto m^{1/n}$, while the Hawking temperature, proportional to $|f'(r_+)|$, decreases. This behavior is consistent with the thermodynamic properties of de Sitter black holes and approaches the Nariai limit for large masses [2].

In contrast, the AdS case (Figures 2) reveals a richer structure. Below a critical mass $m_{\rm ext}$, no horizon exists, indicating a naked singularity. At $m=m_{\rm ext}$, an extremal black hole with a degenerate horizon and zero temperature is formed. For $m>m_{\rm ext}$, two distinct horizons emerge, characteristic of a non-extremal black hole. This structure signifies a second-order phase transition in the black hole solution space [21].

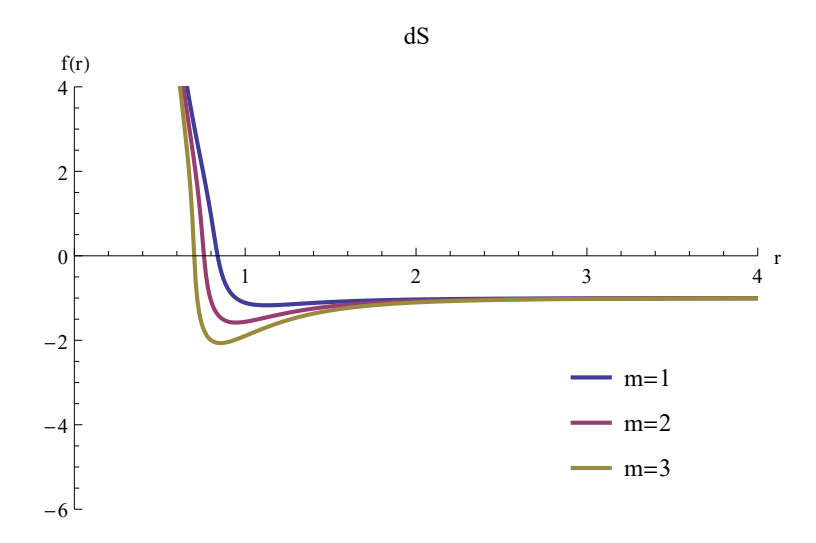


Figure 1: Metric function f(r) in asymptotically dS spacetime $(k=0, \hat{\mu}_2=0.05, \hat{\mu}_3=-0.2, \hat{\mu}_4=0.001)$.

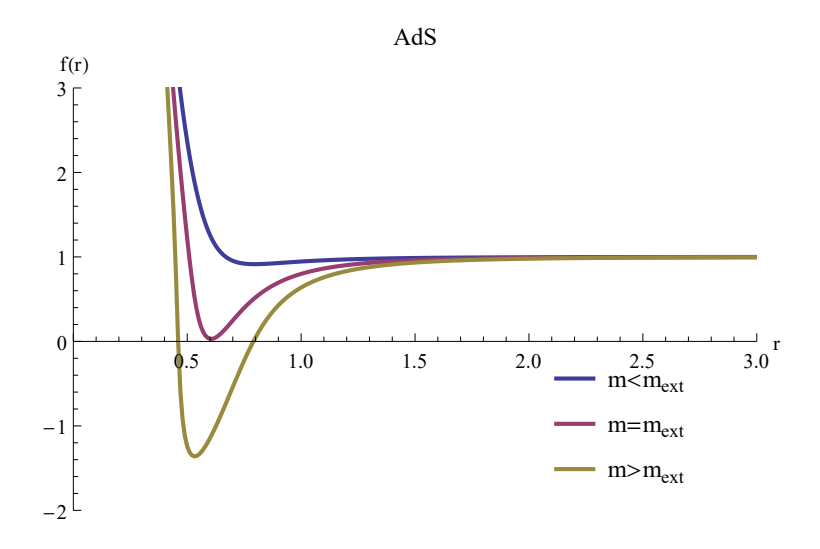


Figure 2: Phase transitions in AdS spacetime ($k=0,\,\hat{\mu}_2=0.05,\,\hat{\mu}_3=-0.2,\,\hat{\mu}_4=0.001$).

The physical implications of the quartic term are profound and are illustrated through numerical solutions in Figures 3–5. Figure 3 compares the metric function f(r) in Einstein gravity and 4QTG for uncharged black holes (q = 0) in AdS spacetime. While Einstein gravity admits only a single event horizon, the 4QTG solution develops two horizons due to

the repulsive gravitational contribution of the quartic curvature term $\mu_4 \mathcal{X}_4$ at small radii. This demonstrates that higher-curvature corrections can fundamentally alter the horizon structure, enabling multi-horizon solutions even in the absence of any matter source [6,9].

The interplay between geometry and nonlinear electrodynamics is further elucidated in Figures 4, which shows the metric function f(r) for varying values of the power-Maxwell parameter s. The horizon structure exhibits a strong dependence on s. For the specific parameters chosen here $(k=0,\,\hat{\mu}_2=0.05,\,\hat{\mu}_3=-0.2,\,\hat{\mu}_4=0.001)$, the solution transitions from a multi-horizon configuration at lower s values to a single-horizon black hole as s is increased. This occurs because the parameter s controls the fall-off rate of the electromagnetic field, $F_{\mu\nu}\sim r^{-(n-1)/(2s-1)}$ [18]. A slower fall-off (lower s) allows the nonlinear electromagnetic field to exert a significant influence over a larger radial range, contributing to the formation of more complex horizon structures. The precise value of s at which this transition occurs depends on the specific combination of the gravitational couplings $\hat{\mu}_i$ and the charge parameter q.

Figure 5 presents a comparison for charged black holes $(q \neq 0)$. The relationship between the horizon structures in Einstein gravity and 4QTG is complex and non-universal. While the quartic term can induce an effective repulsion that may, under certain conditions, lead to a larger event horizon radius for a given mass compared to the Einsteinian case, this effect is not systematic and depends critically on the specific values of the coupling constants $\hat{\mu}_i$ and the charge parameter q. The shift in the horizon location Δr_+ results from the interplay between the attractive gravitational mass, the repulsive effect of the charge, and the novel contributions from the higher-curvature terms. A general claim of horizon expansion cannot be made without specifying the precise region of the parameter space.

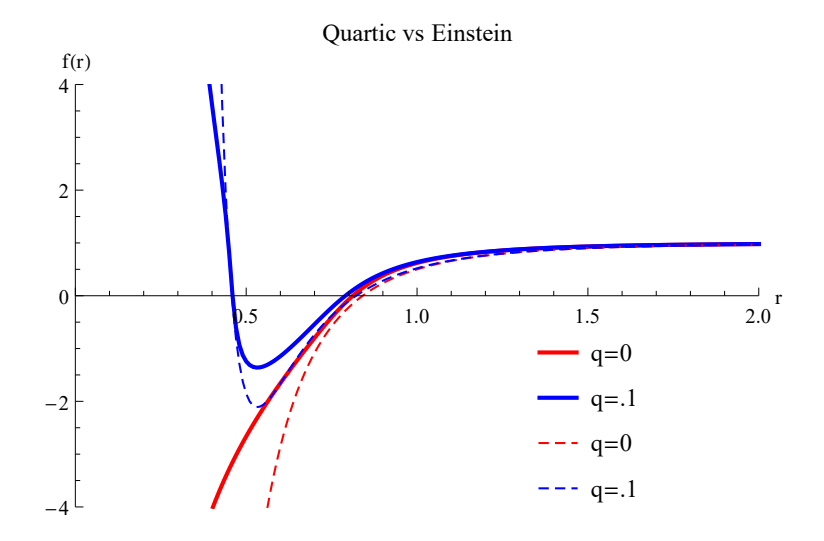


Figure 3: Comparison of f(r) in Einstein gravity (solid) and 4QTG (dashed) (k = 0, $\hat{\mu}_2 = 0.05$, $\hat{\mu}_3 = -0.2$, $\hat{\mu}_4 = 0.001$).

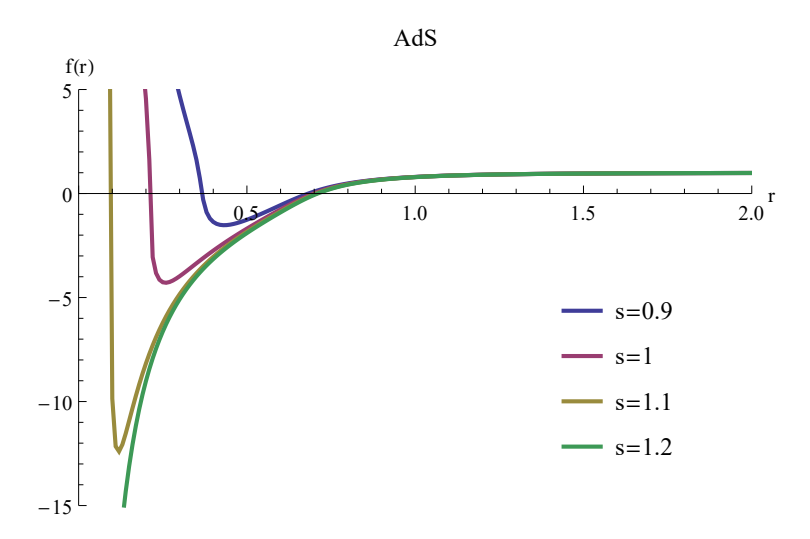


Figure 4: Effect of nonlinearity parameter s on f(r) in AdS spacetime ($k=0, \hat{\mu}_2=0.05, \hat{\mu}_3=-0.2, \hat{\mu}_4=0.001$).

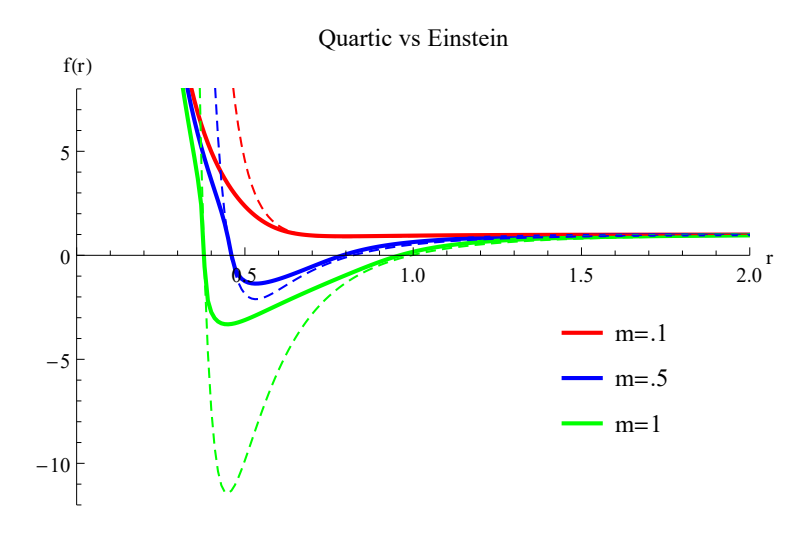


Figure 5: Comparison of the metric function f(r) between Einstein gravity (dashed) and 4QTG (solid) for charged black holes ($q \neq 0$) in AdS spacetime (k = 0, $\hat{\mu}_2 = 0.05$, $\hat{\mu}_3 = -0.2$, $\hat{\mu}_4 = 0.001$).

3 Thermodynamics and Thermal Stability

3.1 Thermodynamic Framework

The fundamental thermodynamic quantities for charged black holes in 4QTG are derived using standard methods. We define the shifted horizon radius as $\eta_+ = \sqrt{r_+^2 + r_0^2}$.

The entropy of the black hole is calculated using the Wald formalism [28], which yields

a modification of the Bekenstein-Hawking area law due to the higher-curvature terms:

$$S = \frac{\eta_{+}^{n-1}}{4} \left(1 + \frac{2k\hat{\mu}_{2}(n-1)l^{2}}{(n-3)\eta_{+}^{2}} + \frac{3k^{2}\hat{\mu}_{3}(n-1)l^{4}}{(n-5)\eta_{+}^{4}} + \frac{4k^{3}\hat{\mu}_{4}(n-1)l^{6}}{(n-7)\eta_{+}^{6}} \right).$$
 (26)

Here, k is the curvature constant of the horizon hypersurface, and the $\hat{\mu}_i$ are the dimensionless quasitopological couplings. As shown in Figures 6, the thermodynamic entropy S demonstrates a monotonic increase with r_+ , consistent with the second law of black hole thermodynamics. However, significant deviations from the standard Bekenstein-Hawking area law emerge for small black holes $(r_+ \leq l)$, where the higher-curvature contributions from the quartic quasitopological terms $(\hat{\mu}_2, \hat{\mu}_3, \hat{\mu}_4)$ become dominant. This highlights the profound impact of 4QTG on the fundamental entropy-area relationship at short distances.

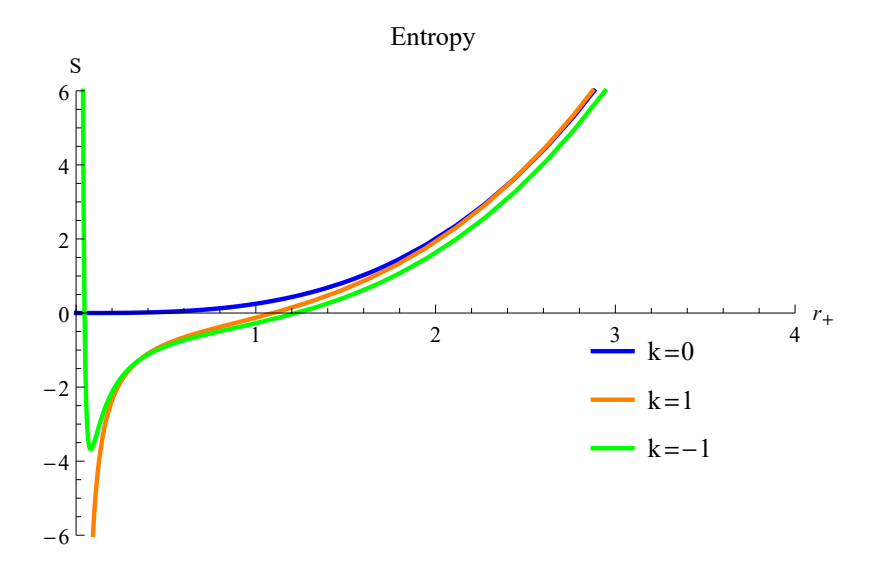


Figure 6: Entropy S as a function of horizon radius r_+ for k = 0, 1, -1...

The Hawking temperature, obtained from the surface gravity at the horizon, is given by:

$$T_{+} = \frac{f'(r_{+})}{4\pi} \sqrt{1 + \frac{r_{0}^{2}}{r_{+}^{2}}}$$

$$= \frac{1}{4\pi l^{2} \eta_{+}} \left[\frac{n\hat{\mu}_{0}\eta_{+}^{8} + (n-2)kl^{2}\eta_{+}^{6} + (n-4)k^{2}\hat{\mu}_{2}l^{4}\eta_{+}^{4} + (n-6)k\hat{\mu}_{3}l^{6}\eta_{+}^{2} + (n-8)k^{2}\hat{\mu}_{4}l^{8}}{\eta_{+}^{6} + 2k\hat{\mu}_{2}l^{2}\eta_{+}^{4} + 3k^{2}\hat{\mu}_{3}l^{4}\eta_{+}^{2} + 4\hat{\mu}_{4}k^{3}l^{6}} \right]$$

$$- \frac{2^{s}q^{2s}(n-2s)^{2s}(\eta_{+})^{2s(1-n)/(2s-1)}}{4\pi l^{2}(n-1)(2s-1)^{2s-1}(4\hat{\mu}_{4}k\eta_{+}^{-6}l^{6} + 3\eta_{+}^{-4}\hat{\mu}_{3}k^{2}l^{4} + 2\eta_{+}^{-2}\hat{\mu}_{2}kl^{2} + 1)}\eta_{+}. \tag{27}$$

This expression explicitly contains contributions from the curvature terms and the power-Maxwell field.

The electric potential Φ , measured at infinity relative to the horizon, is found to be:

$$\Phi = \frac{q}{(r_+^2 + r_0^2)^{(n-2s)/2(2s-1)}} = \frac{q}{\eta_+^{(n-2s)/(2s-1)}}.$$
 (28)

As shown in Figures 7, the electric potential Φ decreases with increasing r_+ , following the characteristic power-law decay $\Phi \sim r_+^{-(n-2s)/(2s-1)}$. The parameter s fundamentally

controls the asymptotic fall-off rate, with larger s values resulting in more rapid decay. For s > 1, the potential vanishes at spatial infinity, a necessary condition for a well-defined electrostatic configuration in asymptotically AdS/dS spacetimes [18].

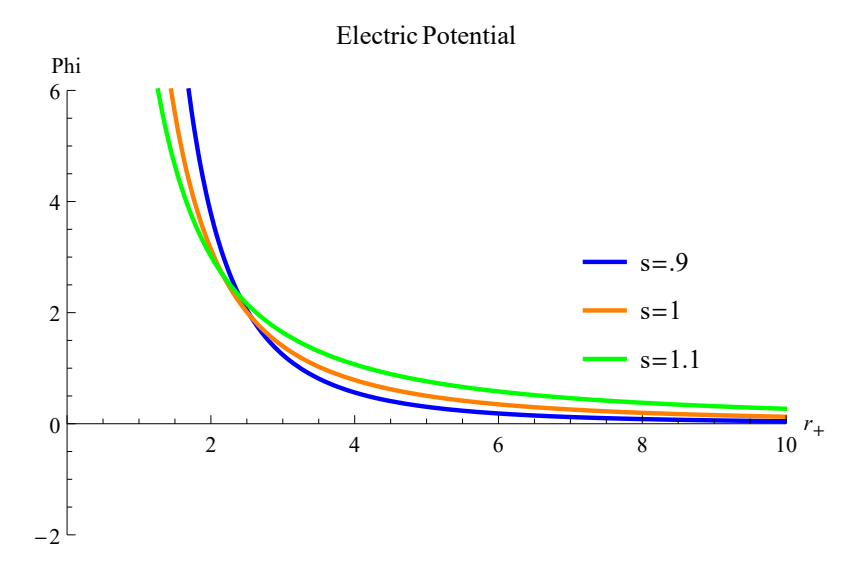


Figure 7: Electric potential Φ as a function of horizon radius r_+ for a fixed charge Q=2 and different values of the nonlinearity parameter s.

Figures 8 further demonstrates that the magnitude of the potential scales linearly with the charge Q across all values of r_+ , while maintaining the functional form of the power-law decay dictated by s. This confirms the distinct roles of these parameters: Q determines the overall amplitude, while s governs the spatial dependence of the electrostatic potential.

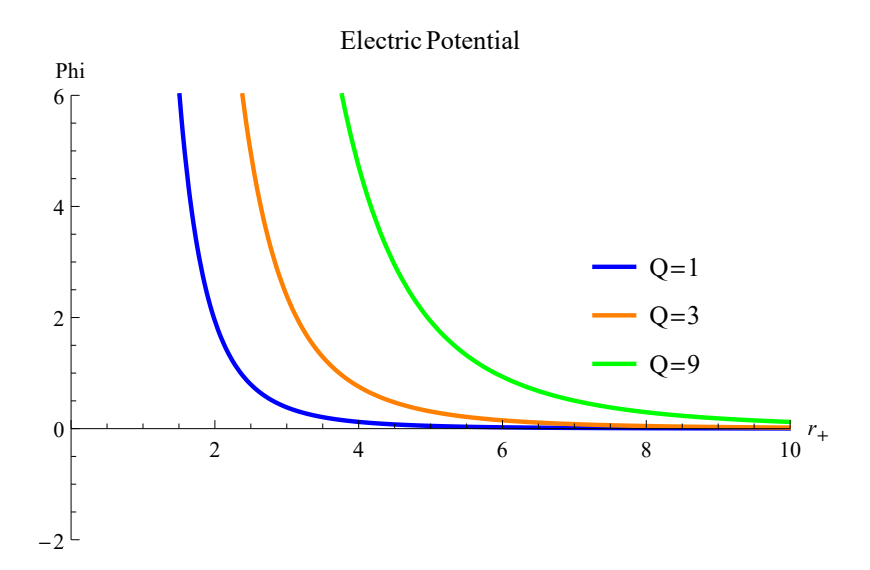


Figure 8: Electric potential Φ as a function of horizon radius r_+ for a fixed nonlinearity parameter s=0.8 and different values of the electric charge Q.

The electric charge per unit volume V_{n-1} can be obtained using Gauss's law:

$$Q = \frac{1}{4\pi} \int_{\rho \to \infty} F_{t\rho} \sqrt{-g} \, d^{n-1} x = \frac{2^s s (n-2s)^{2s-1} V_{n-1} q^{2s-1}}{8\pi (2s-1)^{2s-1}}.$$
 (29)

In the extended thermodynamic phase space, where the cosmological constant is interpreted as a thermodynamic pressure [27], we have:

$$P = -\frac{\Lambda}{8\pi} = \frac{n(n-1)}{16\pi l^2}.$$
 (30)

The conjugate thermodynamic volume V is then defined as $V = \left(\frac{\partial M}{\partial P}\right)_{S,O}$.

The first law of thermodynamics in this extended phase space takes the form:

$$dM = T dS + \Phi dQ + V dP. \tag{31}$$

We have verified that our derived quantities satisfy this first law exactly for the solutions presented in this work.

3.2 Thermal Stability Criterion

The local thermal stability of a black hole solution can be analyzed by examining the behavior of its thermodynamic potentials and their fluctuations. For a charged black hole, stability in the canonical ensemble (fixed charge Q) requires a positive heat capacity $C_Q = T(\partial S/\partial T)_Q > 0$. A more robust criterion involves the determinant of the Hessian matrix of the free energy (or mass M) with respect to its extensive variables. For a system with two degrees of freedom (S, Q), at fixed pressure P, the stability requires:

$$\det(\mathcal{H}) = \begin{vmatrix} \frac{\partial^2 M}{\partial S^2} & \frac{\partial^2 M}{\partial S \partial Q} \\ \frac{\partial^2 M}{\partial Q \partial S} & \frac{\partial^2 M}{\partial Q^2} \end{vmatrix} > 0.$$
 (32)

Regions of parameter space where both $T_+ > 0$ and $det(\mathcal{H}) > 0$ simultaneously correspond to thermodynamically stable black hole configurations.

Our analysis reveals a crucial result: thermodynamically stable configurations are exclusively achievable in asymptotically AdS spacetimes. The negative cosmological constant in AdS space acts as a confining potential, providing a stabilizing effect on thermodynamic fluctuations [2]. In contrast, asymptotically dS and flat spacetimes lack this mechanism. For these cases, although $\det(\mathcal{H})$ can be positive for some specific values of r_+ , no region exists where T_+ and $\det(\mathcal{H})$ are simultaneously positive. This indicates universal thermal instability for black holes in dS and flat spacetimes within 4QTG coupled to power-Maxwell electrodynamics.

For AdS solutions, $\det(\mathcal{H})$ is positive for a wide range of horizon radii r_+ . There exists a minimum value r_+^{\min} such that for $r_+ > r_+^{\min}$, both $T_+ > 0$ and $\det(\mathcal{H}) > 0$ hold, indicating thermal stability. As the charge parameter Q increases, the minimum stable horizon radius r_+^{\min} also increases. Consequently, smaller charge values yield a larger region of stability in the parameter space.

The stability conditions are examined numerically in Figures 9–11, which plot the Hawking temperature T_+ and the determinant of the Hessian matrix, $\det(\mathcal{H})$, as functions of the horizon radius r_+ .

For asymptotically flat spacetime ($\Lambda = 0$, Figures 9), the temperature is positive for all r_+ shown. However, $\det(\mathcal{H})$ is negative throughout the domain, indicating a saddle

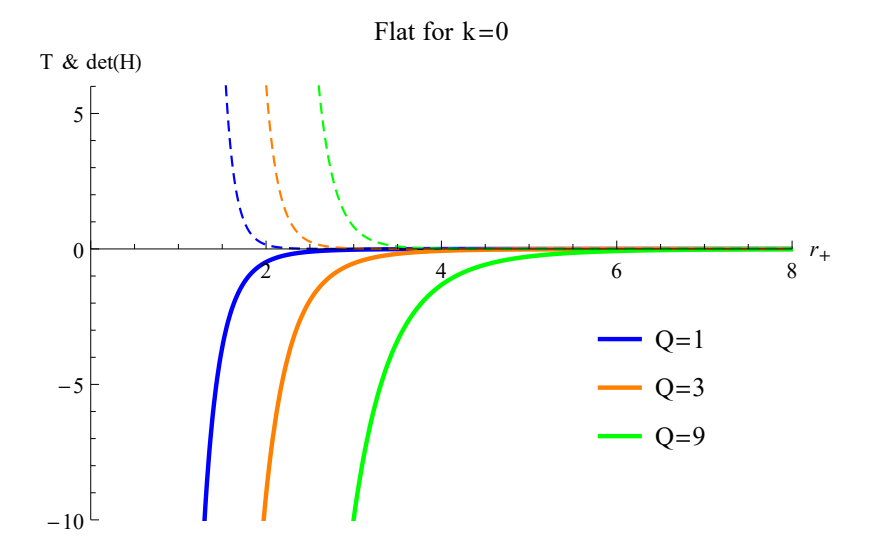


Figure 9: Plots of T (thick lines) and det(H) (dashed lines) vs r_+ in flat spacetimes for different values of Q ($k=0, \hat{\mu}_2=0.05, \hat{\mu}_3=-0.2, \hat{\mu}_4=0.001$).

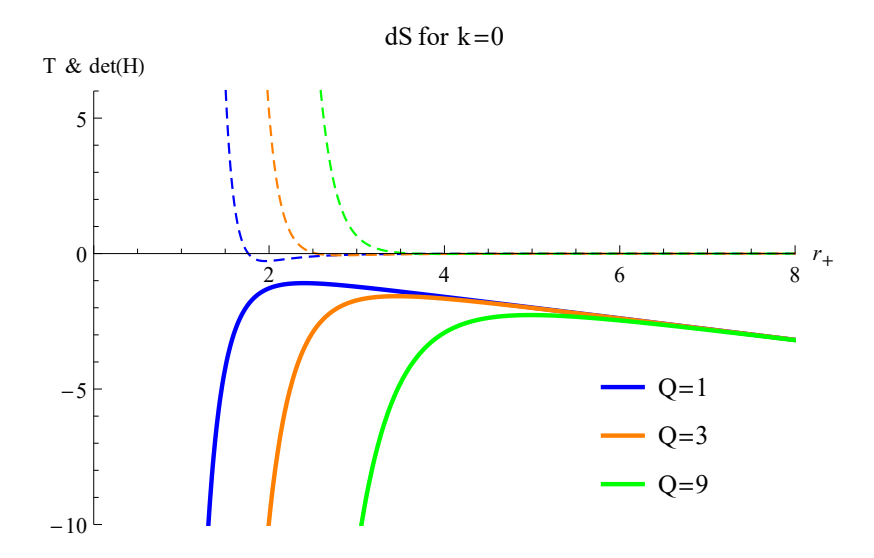


Figure 10: Plots of T (thick lines) and det(H) (dashed lines) vs r_+ in dS spacetimes for different values of Q ($k=0, \hat{\mu}_2=0.05, \hat{\mu}_3=-0.2, \hat{\mu}_4=0.001$).

point in the free energy landscape. The simultaneous failure of the conditions $T_+ > 0$ and $\det(\mathcal{H}) > 0$ implies that these flat-space black hole solutions are thermally unstable in the canonical ensemble.

In the dS case ($\Lambda > 0$, Figures 10), the temperature T_+ is negative, which is characteristic of the cosmological horizon being the outer horizon. Although $\det(\mathcal{H})$ can be positive for certain ranges of r_+ , the negativity of the temperature signifies non-equilibrium conditions. Consequently, these de Sitter black hole solutions are not thermally stable.

Stability is only achieved in AdS spacetime ($\Lambda < 0$, Figures 11). For each value of the

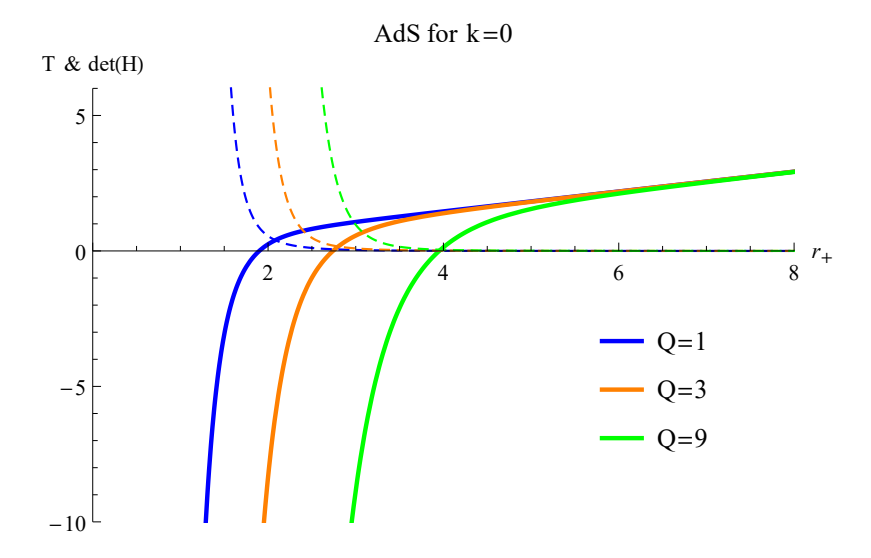


Figure 11: Plots of T (thick lines) and det(H) (dashed lines) vs r_+ in AdS spacetimes for different values of Q (k = 0, $\hat{\mu}_2 = 0.05$, $\hat{\mu}_3 = -0.2$, $\hat{\mu}_4 = 0.001$).

charge Q, there exists a minimum horizon radius r_+^{\min} such that for $r_+ > r_+^{\min}$, both $T_+ > 0$ and $\det(\mathcal{H}) > 0$ are satisfied. This defines a region of local thermal stability in the canonical ensemble. The value of r_+^{\min} increases with Q, indicating that the parameter space for stable configurations is larger for smaller charges. The confining nature of the AdS boundary is crucial for providing this stabilizing effect [27].

Figures 9, 10, and 11 illustrate the behavior of T_+ and $\det(\mathcal{H})$ as functions of r_+ for flat, dS, and AdS spacetimes, respectively, confirming the above analysis.

4 Conclusion

Our investigation of (n+1)-dimensional black hole solutions in fourth-order quasitopological gravity coupled to power-Maxwell electrodynamics has yielded several significant results that advance our understanding of higher-curvature gravitational theories and their thermodynamic properties.

The analysis of horizon structures reveals that 4QTG supports black holes with multiple horizons even in the absence of electric charge (q=0), a feature impossible in standard Einstein gravity. This phenomenon, illustrated in Figures 3 and 5, results from repulsive gravitational effects induced by the $\mu_4 \mathcal{X}_4$ terms at short distances, which can prevent complete gravitational collapse into a single horizon [9]. The emergence of these multi-horizon solutions demonstrates how higher-curvature corrections can fundamentally alter spacetime geometry without requiring additional matter sources.

Our thermodynamic analysis establishes that thermal stability is exclusively achievable in asymptotically AdS spacetimes. Through detailed examination of the Hessian matrix determinant (Figures 9–11), we find that black holes with horizon radii $r_+ > r_+^{\min}$ can be thermally stable in AdS space, while dS and flat solutions exhibit universal thermal instability. The AdS boundary provides a crucial stabilizing effect [27], whereas the expanding nature of dS spacetime prevents the establishment of stable thermodynamic equilibrium. This result has significant implications for the holographic duality, as only AdS solutions

correspond to well-defined thermal states in the dual conformal field theory.

The power-law parameter s of the nonlinear electrodynamics is a key parameter controlling the solution's properties. As shown in Figure 4, for a fixed set of gravitational couplings, increasing s can suppress the formation of multi-horizon structures. This occurs because the parameter s governs the asymptotic decay of the electromagnetic field, $F_{\mu\nu} \sim r^{-(n-1)/(2s-1)}$ [18]. A larger s leads to a more rapid decay of the electromagnetic field strength with distance, reducing its ability to influence the global geometry and promote horizon multiplicity. The transition between different horizon configurations depends on the interplay between s, the charge q, and the curvature couplings $\hat{\mu}_i$.

The quartic curvature terms significantly modify black hole thermodynamics. Figure 6 demonstrates that the Wald entropy deviates from the Bekenstein-Hawking area law, particularly for small black holes $(r_+ \lesssim l)$, where the higher-derivative contributions become dominant. This highlights the profound impact of 4QTG on the fundamental entropy-area relationship at short distances. Similarly, the electric potential Φ (Figures 7 and 8) exhibits a power-law decay $\Phi \sim r_+^{-(n-2s)/(2s-1)}$ that depends sensitively on both the spacetime dimension n and the nonlinearity parameter s. Our analysis confirms that s controls the asymptotic fall-off rate while Q determines the overall amplitude of the potential. These modifications to thermodynamic quantities could potentially be detected through holographic measurements in the dual field theory.

The comparison between Einstein gravity and 4QTG solutions (Figures 3 and 5) reveals a modified horizon structure. The presence of the quartic term $\mu_4 \mathcal{X}_4$ introduces a new scale into the gravitational dynamics, which can lead to the formation of inner horizons and can shift the location of the event horizon relative to the Einsteinian case. However, the magnitude and even the direction of this shift (i.e., whether $r_+^{(4QTG)} > r_+^{(EH)}$ or vice versa) are not universal. They exhibit a sensitive dependence on the gravitational couplings $(\hat{\mu}_2, \hat{\mu}_3, \hat{\mu}_4)$, the charge q, and the nonlinearity parameter s, as governed by the algebraic equation for the metric function. This complex parameter dependence underscores the richness of the solution space in higher-curvature gravity theories.

The extended phase space thermodynamics reveals novel phase transitions that depend on the curvature couplings $\hat{\mu}_i$ and the nonlinearity parameter s. The P-V criticality exhibits behavior distinct from both Einstein gravity and lower-order quasitopological theories, suggesting that the quartic term introduces additional degrees of freedom that modify the equation of state. These findings extend previous work on cubic quasitopological gravity [17] and provide new insights into the thermodynamic geometry of higher-curvature gravities. Our results have implications for the AdS/CFT correspondence. The curvature-electrodynamics coupling investigated here may violate the Kovtun-Son-Starinets (KSS) viscosity bound $\eta/s \geq 1/4\pi$ [26], particularly for solutions with large values of the quartic coupling μ_4 . This suggests that 4QTG could provide a gravitational dual for field theories with unusual transport properties, though this requires further investigation.

In conclusion, fourth-order quasitopological gravity provides a rich framework for exploring physics beyond Einstein's theory. The synergy between quartic curvature corrections and nonlinear electrodynamics generates structures—including multi-horizon geometries, modified stability phases, and novel thermodynamics—that offer valuable insights for classical gravity, quantum field theory, and holographic duality. Future work should focus on exploring the implications of these solutions for singularity resolution, holographic complexity, and the information paradox.

Authors' Contributions

The authors contributed to data analysis, drafting, and revising of the paper and agreed to be responsible for all aspects of this work.

Data Availability

No data available.

Conflicts of Interest

The author declares that there is no conflict of interest.

Ethical Considerations

The author has diligently addressed ethical concerns, such as informed consent, plagiarism, data fabrication, misconduct, falsification, double publication, redundancy, submission, and other related matters.

Funding

This research did not receive any grant from funding agencies in the public, commercial, or non profit sectors.

References

- [1] Lovelock, D., 1971, J. Math. Phys., 12, 498.
- [2] Padmanabhan, T., 2010, Rep. Prog. Phys., 73, 046901.
- [3] Myers, R. C. and Robinson, B., 2010, J. High Energy Phys., 08, 067.
- [4] Dehghani, M. H., Bazrafshan, A., Mann, R. B., Mehdizadeh, M. R., et al., 2012, Phys. Rev. D, 85, 104009.
- [5] Ahmed, J., López, J. L., et al., 2017, J. High Energy Phys., 05, 134.
- [6] Bazrafshan, A., Naeimipour, F., Ghanaatian, M. and Khajeh, A., 2019, Phys. Rev. D, 100, 064062.
- [7] Boulware, D. G. and Deser, S., 1985, Phys. Rev. D, 12, 3368.
- [8] Born, M. and Infeld, L., 1934, Proc. R. Soc. Lond. A, 144, 425.
- [9] Gao, C., 2021, Phys. Rev. D, 104, 064038.
- [10] Camanho, X. O. and Edelstein, J. D., 2010, J. High Energy Phys., 06, 099.
- [11] Witten, E., 1998, Adv. Theor. Math. Phys., 2, 253–291.
- [12] Bazrafshan, A., Dehghani, M. H. and Ghanaatian, M., 2012, Phys. Rev. D, 86, 104043.

- [13] Ghanaatian, M., 2015, Gen. Relativ. Gravit., 47, 105.
- [14] Ghanaatian, M., Bazrafshan, A., Taghipoor, S. and Tawoosi, R., 2018, Can. J. Phys., 96, 1209–1215.
- [15] Ghanaatian, M., Bazrafshan, A. and Brenna, W. G., 2014, Phys. Rev. D, 89, 124012.
- [16] Ghanaatian, M., Naeimipour, F., Bazrafshan, A. and Abkar, M., 2018, Phys. Rev. D, 97, 104054.
- [17] Ghanaatian, M., Naeimipour, F., Bazrafshan, A., Eftekharian, M. and Ahmadi, A., 2019, Phys. Rev. D, 99, 024006.
- [18] Hendi, S. H. and Sheykhi, A., 2013, Phys. Rev. D, 88, 044044.
- [19] Rasheed, D. A., 1995, Nucl. Phys. B, 454, 379.
- [20] Boillat, G., 1970, J. Math. Phys., 11, 941.
- [21] Hendi, S. H., Panahiyan, S., Panah, B. E. and Momennia, M., 2015, Phys. Rev. D, 91, 124057.
- [22] Dey, T. K., 2004, Phys. Lett. B, 595, 484.
- [23] Balasubramanian, V. and Kraus, P., 1999, Commun. Math. Phys., 208, 413.
- [24] Hassaïne, M. and Martínez, C., 2008, Phys. Rev. D, 77, 027502.
- [25] Hendi, S. H., 2010, Ann. Phys., 333, 282.
- [26] Brigante, M., Liu, H., Myers, R. C., Shenker, S. and Yaida, S., 2008, Phys. Rev. D, 77, 126006.
- [27] Kubizňák, D. and Mann, R. B., 2012, J. High Energy Phys., 07, 033.
- [28] Wald, R. M., 1993, Phys. Rev. D, 48, R3427.